Supplementary information

EVOLUTION OF DENSITY OF STATES

Figure S1 shows the evolution of the total density of states (DOS) as a function of the number, m, of STO capping layers in STO(001)/2LAO/mSTO samples. While the first layer has the dominating effect of reducing the band gap by 1.2 eV, a second STO layer leads to a clear band overlap and an enhancement of the DOS at the Fermi level.

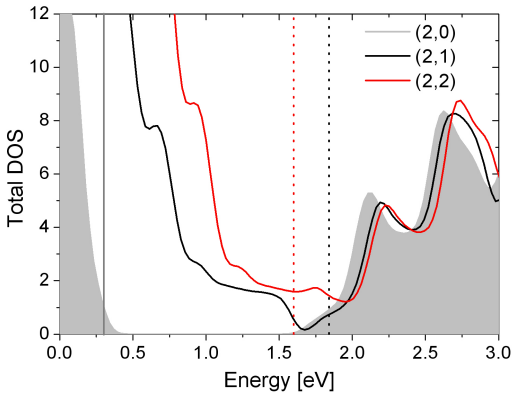

FIG. 1: **Total density of states of STO(001)/2LAO/mSTO.** By adding a STO capping layer, the band gap of STO(001)/2LAO is reduced by 1.2 eV. Further capping layers lead to an increase of DOS at the Fermi level.

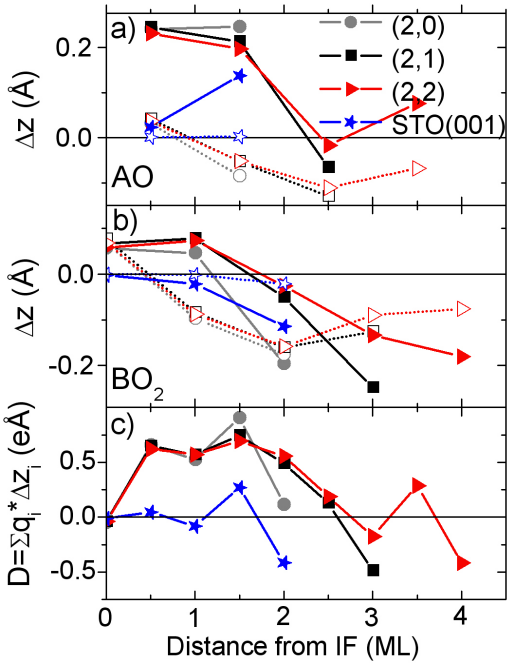

FIG. 2: **Ionic relaxations in STO(001)/2LAO/mSTO and the bare STO(001)-surface.** Vertical displacements Δz with respect to the bulk position in the (a) AO and (b) BO_2 layers, (c) layer-resolved dipole moments as a function of the distance from the interface (IF) TiO_2-layer. The filled (open) symbols mark cation (anion) relaxations. (n, m) denotes the number n of LAO and m of STO layers in the respective system.

IONIC RELAXATIONS

Figure S2 shows the calculated layer resolved ionic displacements in STO(001)/2LAO/mSTO. Additionally, the relaxations of a STO(001)-surface are plotted. The relaxation pattern in the capping layers bears a striking resemblance to the structure of the STO(001) surface, where the total dipole is relatively small $D_{ionic}^{\mathrm{STO(001)}} = -0.19$ eÅ [3]. As mentioned previously, also the electronic structure of the STO(001) surface [1, 2] and the capping layer are similar, in particular a dispersive O $2p$ surface state with maximum at the M-point appears. Due to the small ionic contribution of the capping layer the total dipole moment is not affected appreciably by the capping layer: $D_{ionic}^{(2,0)} = 2.15$ eÅ, $D_{ionic}^{(2,1)} = 2.05$ eÅ, and $D_{ionic}^{(2,2)} = 2.28$ eÅ. The latter turns out to be determined by the total number of LAO layers, *e.g.* $D_{ionic}^{(1,1)} = 1.02$ eÅ, $D_{ionic}^{(2,1)} = 2.05$ eÅ, and $D_{ionic}^{(3,1)} = 3.30$ eÅ.

TWO-BAND FITTING RESULTS

For every electronic band n, that contributes to conductivity, the induced current $\boldsymbol{j_n}$ is given by the electric field $\boldsymbol{E_n}$ times the band conductivity $\boldsymbol{\sigma_n}$, $\boldsymbol{j_n} = \boldsymbol{\sigma_n}\boldsymbol{E_n}$. The band resistivity $\boldsymbol{\rho_n} = \boldsymbol{\sigma_n}^{-1}$ is defined as

$$\boldsymbol{\rho_n} = \begin{pmatrix} \rho_n & -R_n H \\ R_n H & \rho_n \end{pmatrix}, \tag{1}$$

where ρ_n is the longitudinal resistance, R_n the transverse Hall coefficient and H the magnetic field. The *total* resistivity tensor $\boldsymbol{\rho}$, defined as

$$\boldsymbol{\rho_n} = \begin{pmatrix} \rho & -RH \\ RH & \rho \end{pmatrix}, \tag{2}$$

is given by $\boldsymbol{\rho} = \boldsymbol{\sigma}^{-1} = \left(\sum_n \boldsymbol{\sigma_n}\right)^{-1} = \left(\sum_n \boldsymbol{\rho_n}^{-1}\right)^{-1}$. When only two bands contribute to conductivity, it follows that the total longitudinal and Hall resistances can

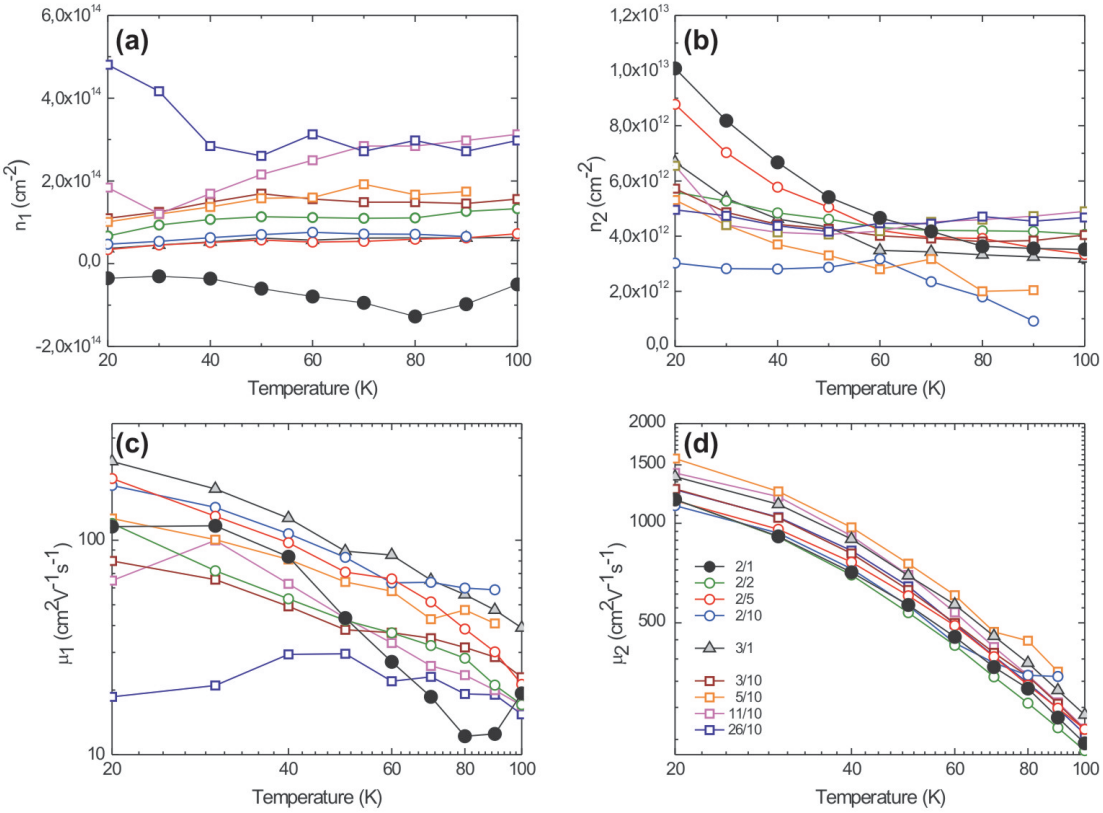

FIG. 3: **Two-band fitting results.** For all STO(001)/nLAO/mSTO samples, the magnetoresistance and Hall effect field dependence were fitted with a two-band model. The fitting provides two carrier densities (a-b) and two mobilities (c-d) for each n/m sample.

be expressed as

$$\rho = \frac{\rho_0 + \rho_\infty \mu^2 H^2}{1 + \mu^2 H^2}, \tag{3}$$

$$R_H = \frac{R_0 + R_\infty \mu^2 H^2}{1 + \mu^2 H^2}, \tag{4}$$

where $R_0 = \left(R_1\sigma_1^2 + R_2\sigma_2^2\right)(\sigma_1+\sigma_2)^{-2}$, $R_\infty = R_1R_2\left(R_1+R_2\right)^{-1}$, $\mu = \left(R_1+R_2\right)\sigma_1\sigma_2\left(\sigma_1+\sigma_2\right)^{-1}$, $\rho_0 = (\sigma_1+\sigma_2)^{-1}$, and $\rho_\infty = \left(R_1^2\sigma_2^{-1} + R_2^2\sigma_1^{-1}\right)\left(R_1+R_2\right)^{-2}$.

The band conductivities are given by $\sigma_{1,2} = |n_{1,2}|\,\mu_{1,2}$ and the band Hall resistivities by $R_{1,2} = (n_{1,2})^{-1}$, where n is negative for electrons (negative curvature in the band dispersion relation) and positive for holes (positive band curvature).

Equations (3) and (4) were fitted simultaneously to the measured sheet resistance and Hall resistance by means of a least square fitting routine. The resistivity data was symmetrized (average over values at positive and negative fields) in order to exclude a transverse resistance contribution to the longitudinal resistance. The Hall resistivity was anti-symmetrized (difference between values at positive and negative fields) in order to exclude longitudinal components. All the different samples could be fitted within the experimental error bars. The results for all measured STO(001)/nLAO/mSTO samples are shown in Fig. S3.

[1] Kimura, S., Yamauchi, J., Tsukada, M. & Watanabe, S. First principles study on electronic-structure of the (001) surface of $SrTiO_3$. *Phys. Rev. B* **51**, 11049 (1995).

[2] Padilla, J. & Vanderbilt, D. Ab initio study of $SrTiO_3$ surfaces. *Surf. Sci.* **418**, 64–70 (1998).

[3] The dipole moment is determined from the ionic displacements using the formal ionic charges. Although Born effective charges may be more appropriate, we use this approach as a rough estimate of the ionic contribution to the total dipole.